Electron Transfer Kinetics in Purified Reaction Centers from the Green Sulfur Bacterium *Chlorobium tepidum* Studied by Multiple-Flash Excitation†

Noriaki Kusumoto,‡ Pierre Sétif,*,§ Klaus Brettel,§ Daisuke Seo,‡ and Hidehiro Sakurai‡

Department of Biology, School of Education, Waseda University, Nishiwaseda, Shinjuku, Tokyo 169-8050, Japan, and Département de Biologie Cellulaire et Moléculaire, Section de Bioénergétique and CNRS URA 2096, CEA, C.E. Saclay, 91191 Gif sur Yvette, France

Received February 25, 1999; Revised Manuscript Received May 10, 1999

ABSTRACT: Reaction center preparations from the green sulfur bacterium *Chlorobium tepidum*, which contain monoheme cytochrome *c*, were studied by flash-absorption spectroscopy in the near-UV, visible, and near-infrared regions. The decay kinetics of the photooxidized primary donor $P840^+$, together with the amount of photooxidized cytochrome *c*, were analyzed along a series of four flashes spaced by 1 ms: 95% of the $P840^+$ was reduced by cytochrome *c* with a $t_{1/2}$ of ≈65 μs after the first flash, 80% with a $t_{1/2}$ of ≈100 μs after the second flash, and 23% with a $t_{1/2}$ of ≈100 μs after the third flash; after the fourth flash, almost no cytochrome *c* oxidation occurred. The observed rates, the establishment of redox equilibrium after each flash, and the total amount of photooxidizable cytochrome *c* are consistent with the presence of two equivalent cytochrome *c* molecules per photooxidizable P840. The data are well fitted assuming a standard free energy change $\Delta G°$ of −53 meV for electron transfer from one cytochrome *c* to $P840^+$, $\Delta G°$ being independent of the oxidation state of the other cytochrome *c*. These observations support a model with two monoheme cytochromes *c* which are symmetrically arranged around the reaction center core. From the ratio of menaquinone-7 to the bacteriochlorophyll pigment absorbing at 663 nm, it was estimated that our preparations contain 0.6−1.2 menaquinone-7 molecules per reaction center. However, no transient signal due to menaquinone could be observed between 360 and 450 nm in the time window from 10 ns to 4 μs. No recombination reaction between the primary partners $P840^+$ and A_0^- could be detected under normal conditions. Such a recombination was observed ($t_{1/2} \approx 19$ ns) under highly reducing conditions or after accumulation of three electrons on the acceptor side during a series of flashes, showing that the secondary acceptors can stabilize three electrons. From our data, there is no evidence for involvement of menaquinone in charge separation in the reaction center of green sulfur bacteria.

The photosynthetic reaction center (RC)[1] of green sulfur bacteria belongs to the group of iron−sulfur type RCs. This group comprises photosystem I (PSI) of plants, algae, and cyanobacteria, and the RCs of heliobacteria (PS-H) and green sulfur bacteria (PS-C). All these RCs contain iron−sulfur clusters which serve as the terminal electron acceptors and can reduce soluble ferredoxin. The two large polypeptides that make up the RC cores show substantial sequence homologies among PSI, PS-H, and PS-C. Whereas in PSI the two core polypeptides are different, but closely related (heterodimer), the cores of PS-C and PS-H are homodimers, i.e., composed of two identical polypeptides (*1*−*3*). The consequences of heterodimeric versus homodimeric RCs for the efficiency of photosynthetic energy conversion are not yet well understood.

Among the iron−sulfur type RCs, PSI is most thoroughly characterized both functionally and structurally (*4*). Functional properties of PS-C were, however, less well characterized mainly due to difficulties in preparing functionally competent complexes (reviewed in refs *5* and *6*). The primary electron donors in PSI, PS-H, and PS-C are special pairs of chlorophyll (Chl) *a* (P700), bacteriochlorophyll (BChl) *g* (P798), and BChl *a* (P840), respectively. On the acceptor side of PSI, the functioning of five electron acceptors, namely, a Chl *a* as the primary acceptor (A_0), a phylloquinone (A_1), and three iron−sulfur clusters (F_A, F_B, and F_X), has been amply documented (reviewed in ref *7*). The primary acceptor A_0 in PS-C is $BChl_{663}$, an isomer of Chl *a*. Heterodimeric PSI binds two phylloquinones, at least one of which participates in electron transfer (*7*). From strong similarities found among PSI, PS-H, and PS-C, it was expected that quinone is serving as an electron acceptor also in the two latter RCs. However, recent data for membranes from heliobacteria have called into question the possibility that a quinone participates in electron transfer in PS-H in a manner similar to that in PSI (*8*, *9*). In PS-C, several photochemically active preparations from different laboratories contained negligible or substoichiometric amounts of quinones (*10*, *11*). However, Kjaer et al. (*12*) recently found that a purified preparation from *Chlorobium vibrioforme*

† This work was supported in part by Grants-in-aid for Scientific Research from the Ministry of Education, Science and Culture, Japan, to H.S. (Grants 08044223, 10044218, and 10640640).

* Corresponding author. Fax: +33 1 6908 8717. E-mail: setif@dsvidf.cea.fr.

‡ Waseda University.

§ C.E. Saclay.

[1] Abbreviations: ^{3}BChl, triplet state of bacteriochlorophyll; ^{3}Car, triplet state of carotenoid; BChl, bacteriochlorophyll; Chl, chlorophyll; cyt, cytochrome; DTT, dithiothreitol; E_m, midpoint redox potential; fwhm, full width at half-maximum; mPMS, 1-methoxy-5-methylphenazinium methyl sulfate; PS-C, reaction center of green sulfur bacteria; PS-H, reaction center of heliobacteria; PSI, photosystem I reaction center; RC, reaction center.

10.1021/bi990452s CCC: $18.00
Published on Web 08/24/1999

contains 1.7 molecules of menaquinone-7 per RC, and observed a semiquinone-like signal from EPR spectroscopy like that found in PSI after photoaccumulation. Such signals had already been reported in green sulfur bacterial membrane preparations as well as in some purified PS-C preparations (*13*). Results from special TRIPLE spectroscopy suggest that a 2-methylnaphthoquinone radical could photoaccumulate at 205 K in a membrane fraction from *Chlorobium limicola* (*14*). However, electron transfer kinetic measurements have not provided to this point any clear evidence for the involvement of quinone in the main electron transfer pathway in PS-C. With regard to iron−sulfur clusters, the presence of two clusters in PS-C (equivalent to F_A and F_B of PSI) was easily detected by EPR spectroscopy (*10, 15, 16*, and references therein), but only small signals ascribed to F_X have been observed (*10, 15, 17*).

Purified PS-C preparations from several laboratories bind about two molecules of monoheme type cyt *c* per RC (*18*; reviewed in ref *6*), in contrast to PSI and PS-H which bind no cyt. Both cyt *c* molecules in PS-C can be oxidized by $P840^+$, and some controversial kinetics of the reaction were reported (see the Discussion). A model was presented in which two cyt *c* molecules are arranged around the primary donor P840 (*19*), but detailed kinetic measurements for proving this model are still lacking.

In this work, we performed a detailed kinetic study of electron transfer in purified PS-C from the green sulfur bacterium *Chlorobium tepidum* at room temperature. This was done by flash-absorption spectroscopy in the nanosecond to millisecond time range, using in many cases multiple-flash excitations, on one hand for probing the detailed kinetics of bound cyt *c* oxidation by $P840^+$ and on the other hand for characterizing the photoaccumulation of reduced acceptors and searching for a quinone contribution.

MATERIALS AND METHODS

Purification and Characterization of Reaction Centers. Photochemically active PS-C complexes were prepared from *C. tepidum* as previously described (*15*) with some modifications. Briefly, the concentration of dithionite in the media used for washing and breaking cells and for sucrose density gradient centrifugation was decreased to 0.5 mM, and cells were disrupted with a French pressure cell three times at 140 MPa instead of with a BioNebulizer. Dithionite was omitted from the media used for subsequent DEAE-cellulose and hydroxyapatite column chromatography, and 5 mM glucose, 0.25% (v/v) ethanol, 2 mM $MgCl_2$, glucose oxidase (1.25 units/mL), and catalase (5.2×10^{-3} unit/mL) were added to the media. The effluent from the DEAE Bio-Gel A column was diluted, and treated in two different ways, yielding Prep-A and Prep-B. For Prep-A, the hydroxyapatite column was 1−1.5 cm in height and the column was equilibrated with a buffer containing 20 mM HEPES (pH 7.0), 10 mM potassium phosphate buffer (pH 7.0), 2 mM $MgCl_2$, 0.1 mM EDTA, 0.1% Triton X-100, and 2 mM dithiothreitol. For Prep-B, the hydroxyapatite column was 2.5−3 cm in height and the column was equilibrated without potassium phosphate buffer. The diluted DEAE effluents were applied to the columns, which were washed with 5−10 column volumes of the respective equilibration buffers, and PS-C was finally eluted with a buffer containing 80 mM potassium phosphate (pH 7.0). Prep-B was similar to the preparation described in ref *15*; the purified PS-C was composed of five different polypeptides, and contained about 1.5 photooxidizable cyt *c* molecules per photoactive P840 (see the Results). PS-C of Prep-A contained about 2 photooxidizable cyt *c* molecules per photoactive P840 (see the Results) and several other polypeptides as minor components in addition to the five polypeptides found in Prep-B. It was shown by N-terminal amino acid sequencing that the cyt *c* moiety of these preparations corresponds to the monoheme cyt *c* that was first identified in ref *18* and was found in another RC complex from *C. tepidum* (*20*). Both types of preparations had absorbance maxima in the near-infrared region at 811−814 nm, and $A_{\approx 810}$ represents the absorbance at the maximum. Both preparations contained FMO protein, but the content per RC was lower in Prep-B than in Prep-A. The menaquinone-7 content was determined according to the method described in ref *12* by extraction with organic solvent and analysis with a high-pressure liquid chromatograph equipped with a photodiode array for absorption spectrum measurements of peak fractions monitored at 270 nm (HP1100, Hewlett-Packard). Pure menaquinone-7 was purified from *C. tepidum* for use as a standard. A chromatogram similar to that observed in ref *12* was obtained with a large peak due to $BChl_{663}$ and a well-defined peak due to menaquinone-7. The relative amounts of $BChl_{663}$ and menaquinone-7 were determined from their peak areas measured at 270 nm, by assuming absorption coefficients of 22 and 16.8 mM^{-1} cm^{-1} at 270 nm for both species, respectively (*12*). Menaquinone to $BChl_{663}$ ratios of 0.09−0.13 were thus determined. Values of 6 (*21*) and 9 (*12*) were previously reported for the $BChl_{663}$/P840 molar ratio in PS-C preparations. If the preceding values of the $BChl_{663}$/P840 ratio are assumed, our measurements are consistent with a menaquinone-7/P840 molar ratios of 0.6−0.8 and 0.8−1.2, respectively. All procedures for the preparation of RC complexes and kinetic measurements were carried out under strictly anaerobic conditions.

Flash-Absorption Spectroscopy. Different setups were used for flash-absorption measurements at various wavelengths and with different time resolutions. All measurements were performed at 296 K. The transients were fitted to a multiexponential decay using a Marquardt least-squares algorithm. The standard reaction mixture contained 50 mM Tris-HCl (pH 8.0), 0.1 mM EDTA, 2.5 mM $MgCl_2$, 0.1% Triton X-100, and the indicated PS-C preparation.

Kinetics of $P840^+$ decay were recorded mostly at 970 and 1150 nm, two wavelengths at which the measuring light has no actinic effect. $P840^+$ exhibits a broad absorption band around 1150 nm with an estimated maximal ϵ of 21 mM^{-1} cm^{-1} at 1157 nm (*22*). The wavelength of 970 nm [$\epsilon \approx 4$ mM^{-1} cm^{-1} (*22*)] was used in some experiments due to the availability of a laser diode which allows measurement of absorbance kinetics with a nanosecond time resolution. The samples were excited at 90° to the measuring beam by various sources. Many experiments involved one or two excitations; these were provided by two similar ruby laser flashes (Quantel) separated by an adjustable delay (694.3 nm, duration of 25 ns, energy ≈ 110 and 160 mJ for the two flashes, respectively). For three- and four-flash experiments, a Xe flash without any filter was also used for second and third flash excitation, respectively (duration of 5 μs).

Under our experimental conditions, both the ruby lasers and the Xe flash were found to saturate the photochemistry of PS-C. For four-flash experiments, the last flash was provided by a frequency-doubled Nd:YAG laser (532 nm, duration of 300 ps, 1.5 mJ/cm^2 at the surface of the sample cuvette) which was found to induce charge separation in about 90% of the photoactive PS-C. In most experiments, exciting flashes were attenuated as indicated in the Results and in the figure legends. For signal averaging, one series of flashes was given every 15 s. It was determined that such a repetition time was sufficient to allow complete relaxation of RC to their initial redox state. For measurements taken at 550, 560, 1150, and 970 nm with a microsecond time resolution, an opal glass was inserted in the exciting laser beams in front of the sample to homogenize excitation. The laser energies given above were measured without opal glass so that the laser energies effectively received by the samples are smaller than indicated (by a factor of 2−3).

For measurements taken at 1150 nm, the measuring light was provided by a 200 W tungsten−halogen lamp and the wavelength was selected with interference filters with a 35 nm bandwidth (fwhm) placed before and after the (1 cm × 1 cm) square cuvette containing the sample. Absorbance changes were detected with a germanium photodiode with a 5 mm diameter [type J16-85P-R05M-HS from EG&G Judson (Montgomeryville, PA)]. The time resolution of the setup was limited by the detecting diode: 4 μs for signal rise (10−90%). If the published spectrum of P840$^+$ around 1150 nm (*22*) with a $\Delta\epsilon$ of 21 mM^{-1} cm^{-1} at 1157 nm and the transmission spectra of our broadband interference filters are assumed, an effective $\Delta\epsilon$ of 18.6 mM^{-1} cm^{-1} can be calculated after integration over the bandwidths of filters. The same setup was also used at 970 nm for characterization of the saturation properties of the different laser sources (interference filters with a 3 nm fwhm).

To measure the kinetics of P840$^+$ on a nanosecond time scale, we used a continuous-wave laser diode emitting at 971 nm (model C86123E from EG&G) as the measuring light source, and a faster detection system [a model FND 100 photodiode from EG&G, a model IV72A amplifier from the Hahn-Meitner Institut Berlin (30 dB, 500 Hz to 1.7 GHz) or HCA from FEMTO Berlin (28 dB, DC-325 MHz), and a model DSA 602A digital oscilloscope with plug-in 11A52 (DC-100 MHz) from Tektronix]. The time resolution of the setup was 5 ns with the Nd:YAG laser as the excitation source. The inner dimensions of the sample cuvette were 10 mm in the direction of the measuring light beam and 2 mm in the direction of the excitation beam.

Flash absorption spectroscopy in the near-UV and blue spectral regions with a time resolution of 5 ns was performed with a setup similar to the one described in refs *9* and *23*. The sample was excited repetitively (1 Hz) with Nd:YAG laser pulses (532 nm, 300 ps duration, up to 10 mJ/cm^2 at the surface of the cuvette). The measuring light was provided by the relatively flat top of a 50 μs Xe flash. Adequate combinations of interference and colored filters placed in the measuring beam before the sample and in front of the detector (FND100Q form EG&G) yielded a spectral bandwidth of 2−8 nm.

Kinetics of cyt *c* oxidation were recorded with a 1 μs time resolution by measuring absorbance changes at 550 and 560 nm and calculating the difference between the two traces.

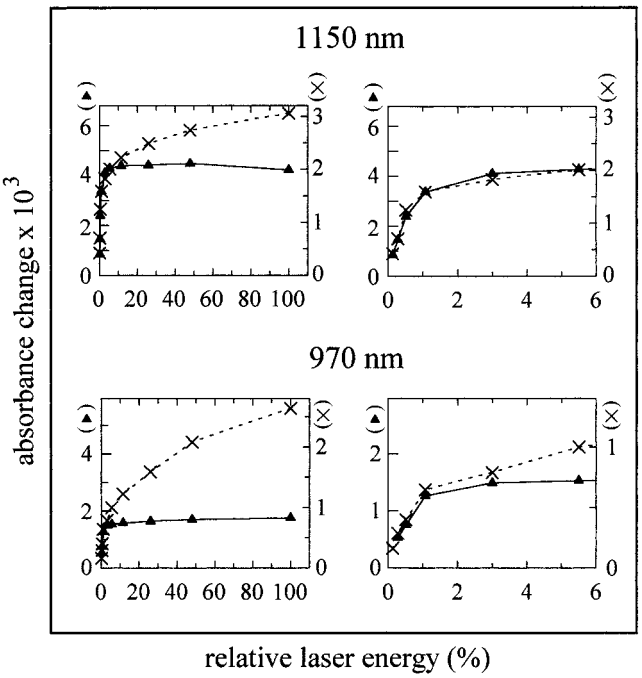

FIGURE 1: Dependence of the initial flash-induced absorbance changes at 1150 and 970 nm upon laser energy for Prep-A (×, right-hand scales) and Prep-B (▲, left-hand scales). The standard reaction mixture contained 1.25 mM DTT, 0.5 mM sodium ascorbate, and 31 nM mPMS for Prep-A ($A_{\approx 810} = 1.15$) and 2 mM dithiothreitol (DTT) and 5 mM sodium ascorbate for Prep-B ($A_{\approx 810} = 1.5$). Flash excitation was provided by a ruby laser whose maximum energy (100%) was 110 mJ. For easier comparison between the two samples, vertical scales have been chosen so that the signal amplitudes at 1150 nm for a laser energy of 1.07% (1.2 mJ) coincide in the plots. This gives a ratio of 2.12 between the left and right *Y*-scales. The same ratio has been used at 970 nm. Each data point corresponds to an average of two to four experiments. The time interval between two flashes was 15 s. See the text for the procedure for determining the initial absorbance changes.

This procedure should correct for the contribution due to the reduction of P840$^+$ and also diminish contributions from carotenoid and chlorophyll triplet states. The same light sources (lasers and Xe flash for excitation and tungsten−halogen lamp for detection) that were used for measurements in the infrared region described above were used. The measuring light was filtered with interference filters with a 3 nm bandwidth, and signals were detected with a silicium photodiode (type S3590-05 from Hamamatsu Photonics). Only a few minutes were necessary for changing the detector (germanium ↔ silicium) while keeping the same geometry of excitation and position of the cuvette so that the same sample could be studied at 1150 nm, and 550 and 560 nm, in an alternate manner, thus allowing reliable comparisons of the absorbance kinetics in both wavelength regions. For these experiments, a shutter was placed in the measuring light beam before the cuvette and was opened 1 ms before the first actinic flash was fired, to decrease the magnitude of the actinic effect of the measuring light. For signal averaging, one series of flashes was given every 15 s.

Dependence of Absorbance Changes at 970 and 1150 nm on Excitation Energy. These experiments were performed with a ruby laser flash (100% energy ≈ 110 mJ) with Prep-A and Prep-B (see above). Figure 1 displays the laser energy dependence of the initial positive absorbance changes at 970

and 1150 nm with these two samples [Prep-A (×) and Prep-B (▲)]. These initial changes were determined from fitting the data with several exponential components (see below), between 10 μs and 10 ms after the flash, and extrapolating them to time zero. Different energy profiles were observed with the two types of preparations. With Prep-B, the amplitude of the flash-induced absorbance change at 1150 nm is rising rapidly with excitation energy, is almost saturated at a laser attenuation of 6% (saturable component), and remains essentially unchanged above 11%. This contrasts with Prep-A, in which the initial rapid rise (up to 6% of the laser energy) is followed by an increase with a smaller slope up to the maximal laser energy (nonsaturable component). Basically the same features were observed at 970 nm with a larger contribution of the nonsaturable component. In Prep-A, the ratios of the amplitude of the nonsaturable component to that of the saturable component (at 100% energy) are about 2.4 and 0.5 at 970 and 1150 nm, respectively. In Prep-B, the corresponding ratio is about 0.15 at 970 nm whereas the amplitude of the nonsaturable component at 1150 nm is so small that it cannot be clearly identified. With both preparations, photooxidation of cyt c_{551} was saturated at about 6% energy (data not shown). Shuvalov and Parson previously reported that formation of the BChl triplet state (^{3}BChl *a*) gives rise to positive absorbance changes above 900 nm (*24*). Our results indicate that the nonsaturable component arises from such triplet states and that it interferes with P840$^+$ absorption measurements (saturable component) much less at 1150 nm than at 970 nm. From our measurements, the $\Delta A_{1150}/\Delta A_{970}$ ratio is 2.8 ± 0.1 and 0.7 ± 0.1 for P840$^+$ and ^{3}BChl *a*, respectively. The wavelength of 1150 nm seems therefore to be a very useful wavelength at which to study P840$^+$ decay due to the large absorption coefficient of this species and the relatively weak contribution of antenna triplet states. The ratio of 2.8 found here for P840$^+$ ($\Delta A_{1150}/\Delta A_{970}$) is significantly smaller than the ratio of about 4.6 that is expected from the spectrum published by Olson et al. (*22*).

For analysis of the decay at either 970 or 1150 nm, a global fit with two exponential components and an offset accounting for longer-lived components was performed at each wavelength for all laser energies with a sample from Prep-A (relatively large ^{3}BChl *a* signal compared to Prep-B). The fit was satisfactory and gave the following results: $t_{1/2}$ = 69 and 394 μs at 1150 nm; $t_{1/2}$ = 59 and 412 μs at 970 nm (not shown). The amplitude of the slower exponential component increased almost linearly with excitation energy (up to the maximal energy of the ruby laser), indicating that it arises mostly from ^{3}BChl *a*. Although the picture is less clear for the faster component, the fact that its amplitude at 1150 nm ($t_{1/2}$ = 69 μs) almost reaches a plateau at about 11.5% laser energy indicates that it corresponds mostly to P840$^+$ decay. However, the 59 μs component obtained at 970 nm exhibits a biphasic behavior versus laser energy, showing that some ^{3}BChl *a* molecules are also decaying with kinetics similar to those of P840$^+$ decay. In summary, it can be concluded that the ^{3}BChl *a* decay is multiphasic with $t_{1/2}$ ranging from tens to hundreds of microseconds (see also ref *25*) and that low and subsaturating laser energies should be used especially with Prep-A to monitor reliably the P840$^+$ decay, even at the favorable wavelength of 1150 nm. Under such conditions, reduction of P840$^+$ by cyt *c* was satisfactorily fitted with a single-exponential phase. Fitting with two exponentials improved the fits only marginally, giving generally halftimes differing by a factor of 2−3. However, these results were not reproducible from experiment to experiment, even using the same sample. It has been checked that this was not due to any aging process, but it can be ascribed to the inherent limitation of data fitting (cross-correlation effects) with two similar decay phases under conditions of a limited signal-to-noise ratio (*26*). When the oxidation kinetics of cyt c_{551} were studied at 550 and 560 nm, signals due to carotenoid triplet states (^{3}Car) were observed. As for ^{3}BChl *a*, the ^{3}Car signals were larger in Prep-A than in Prep-B.

RESULTS

For this study, we performed various flash-absorbance measurements on two different types of RC preparations from *C. tepidum*, namely, Prep-A and Prep-B. These two preparations exhibit different amounts of ^{3}BChl *a* after laser flash excitation, with the higher amount occurring in Prep-A (Figure 1). However, both preparations are highly photoactive, as will be shown further below, and the saturation properties of absorbance changes show that the triplet states observed in the infrared region arise essentially from BChl *a* in the antenna (see Materials and Methods). In the following, we will mostly describe the results obtained with Prep-A, which is considered to be more native with respect to electron transfer from cyt *c* to P840$^+$ (see below), though it appears to contain more disconnected antennae BChl *a* than Prep-B.

Comparison of P840$^+$ Decay Kinetics after the First and the Second Flash. The kinetics of P840$^+$ decay were studied in a Prep-A sample at 1150 nm (Figure 2). The upper part shows the transient recorded after a single flash using a subsaturating excitation energy (1.2 mJ) to minimize ^{3}BChl *a* signals (see Materials and Methods). In a separate two-flash experiment, the transient induced by the second flash (subsaturating energy of 1.7 mJ) was also recorded (Figure 2, lower part). In this last experiment, a higher energy was used for the first flash (fired 1 ms before the second flash) to hit all reaction centers. The decay curves following the initial absorbance increase due to P840$^+$ formation were satisfactorily approximated by a monoexponential component together with a longer-lived absorbance change (fitted as an offset, $t_{1/2}$ > 40 ms; not shown). Halftimes of 62 and 97 μs were found for the first and second flashes, respectively. The very slow component (offset) is larger after the second flash than after the first one (20% of the initial amplitude vs 6%). Because of the 4 μs time resolution of the experiments described here, it can be asked whether a faster component of P840$^+$ decay could have escaped detection. This was first checked by repeating the one-flash experiment at 1150 nm with a Ge photodiode with a smaller area (diameter of 1 mm instead of 5 mm) which allows a 1.5 μs time resolution to be achieved. No evidence for a faster component with a significant amplitude was observed (not shown). Moreover, absorbance change measurements were also performed at 970 nm with a DC-100 MHz bandwidth (inset of Figure 2). It is quite apparent from this experiment that there was no significant decay phase of P840$^+$ with $t_{1/2}$ in the range of 1−10 μs as the observed decay can be ascribed to the ≈60 μs phase. The decay of P840$^+$ has also been probed on a

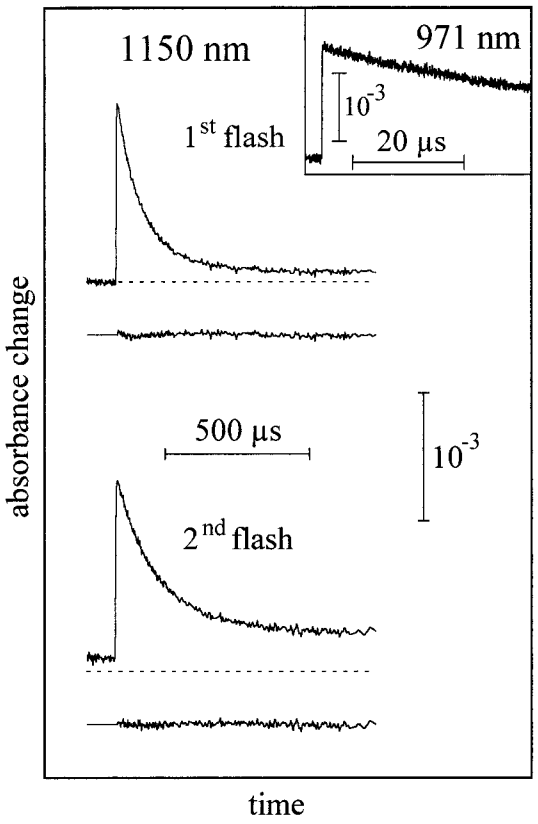

FIGURE 2: Flash-induced absorbance changes measured at 1150 nm. The standard reaction mixture contained Prep-A ($A_{\approx 810} = 1.5$) and 5 mM sodium ascorbate. The upper trace depicts the results of a single-flash experiment. The ruby laser was about 100-fold attenuated (1.2 mJ). The absorbance decay was fitted by a monoexponential component together with an offset parameter to take into account the longer-lived absorbance change: $t_{1/2} = 62.5$ μs, amplitude $= 1.37 \times 10^{-3}$ (94%), and offset amplitude $= 0.087 \times 10^{-3}$ (6%). The lower trace depicts the results of the two-flash experiment with a time interval of 1 ms between flashes. The absorbance change following the second flash is shown together with the baseline preceding the first flash (dotted line). The first flash was provided by a ruby laser with 13 mJ of energy which was sufficient for saturating photochemistry, while the second flash was provided by a second ruby laser with 1.7 mJ of energy. The absorbance decay was fitted as it was for the single-flash experiment: $t_{1/2} = 97$ μs, amplitude $= 1.35 \times 10^{-3}$ (80%), and offset amplitude $= 0.34 \times 10^{-3}$ (20%). The offset was calculated by reference to the baseline before the first flash. Both traces correspond to an average of eight experiments (interval of 15 s). Residuals corresponding to the fits are shown below the respective traces. From saturation curves (see Figure 1), laser energies of 1.2 (flash in the upper trace) and 1.7 mJ (second flash in the lower trace) were expected to trigger photochemical charge separation in about 79 and 85% of the RCs, respectively. The inset shows flash-induced absorbance changes at 971 nm measured with a time resolution of 100 ns. The standard reaction mixture contained Prep-A ($A_{\approx 810} = 4.6$), 5 mM sodium ascorbate, 100 μM sodium dithionite, and 0.5 μM mPMS. Repetitive (1 Hz) excitation flashes at 532 nm ($\approx$0.7 mJ/cm^2) were provided by a 300 ps Nd:YAG laser.

nanosecond time scale under different conditions (see Figures 5 and 8 below).

Comparison of the Kinetics of P840$^+$ Reduction and Cyt c_{551} Oxidation. Flash-induced oxidation kinetics of cyt c_{551} were measured as the difference [$\Delta A_{550} - \Delta A_{560}$, $\Delta A_{(550-560)}$ in the following] for comparison with the kinetics of P840$^+$ decay (Figure 3). Prep-B was used for these experiments, as the triplet signals, both from BChl *a* and from carotenoids,

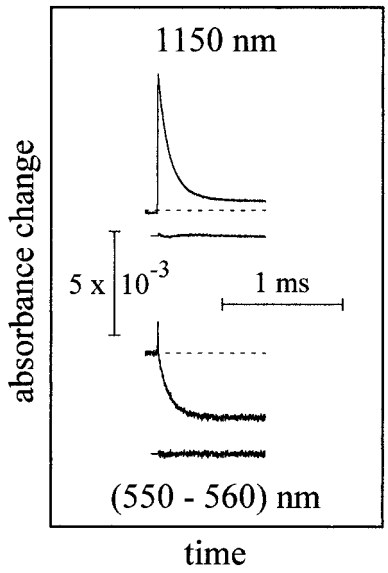

FIGURE 3: Flash-induced absorbance changes measured at 1150 nm (upper part) and 550 nm − 560 nm (lower part). The kinetics shown in the upper and lower parts were obtained from different samples from the same batch of Prep-B ($A_{\approx 810} = 1.5$ and 1.0, respectively). They only differed in the RC concentration, and for an easier comparison, data are shown after normalization to the same concentration ($A_{\approx 810} = 1.0$). The standard reaction mixture contained 0.5 mM sodium ascorbate. The data in the upper part are the average of eight experiments (interval of 15 s); the energy of the ruby laser was saturating (13 mJ). The decay was fitted with one exponential component and an offset parameter: $t_{1/2} = 68$ μs, amplitude $= 5.39 \times 10^{-3}$, and offset amplitude $= 0.52 \times 10^{-3}$. For the lower part, absorbance kinetics were recorded at both 550 and 560 nm and the difference between the signals observed at these two wavelengths is shown. An average of five experiments (interval of 15 s) were carried out at each wavelength. The energy of the ruby laser was 0.8 mJ. Fit parameters were as follows: $t_{1/2} = 63.5$ μs, amplitude $= 3.35 \times 10^{-3}$, and offset amplitude $= -3.10 \times 10^{-3}$. The fitting was started 6 μs after the excitation flash (time zero), but the fit function was extrapolated back to time zero. This was done so that some faster components ascribed to ^{3}Car would not be taken into account (see the text). Residuals corresponding to the fits are shown below the respective traces.

are smaller in this preparation than in Prep-A. On a millisecond time scale, a positive spike was observed in $\Delta A_{(550-560)}$ which can be ascribed to some ^{3}Car which was not completely canceled by subtraction of ΔA_{560} (*25*). The size of this spike increased with excitation flash energy, and a small laser energy of 0.8 mJ was used to minimize its relative contribution. This laser energy elicits charge separation in approximately 60% of the RCs, according to the laser energy dependence of ΔA_{1150} (Figure 1). The spike observed at this energy has completely decayed 5 μs after the flash. The cyt *c* oxidation curve was fitted by a monoexponential decay with a $t_{1/2}$ of 64 μs. For the same sample, the P840$^+$ kinetics were studied at 1150 nm, where a saturating laser energy could be used without inducing large ^{3}BChl *a* signals (Figure 3, top). The decay curve was satisfactorily approximated by a monoexponential decay with a $t_{1/2}$ of 68 μs. The good correspondence in $t_{1/2}$ between the microsecond phases observed in both wavelength regions indicates that these phases reflect the process of P840$^+$ reduction by cyt *c*, as was previously reported (*20*, *27*; see ref *6* for a review).

The measurements at 550−560 nm were taken with a better time resolution than those at 1150 nm (<1 vs 4 μs), thus allowing the existence of a faster microsecond compo-

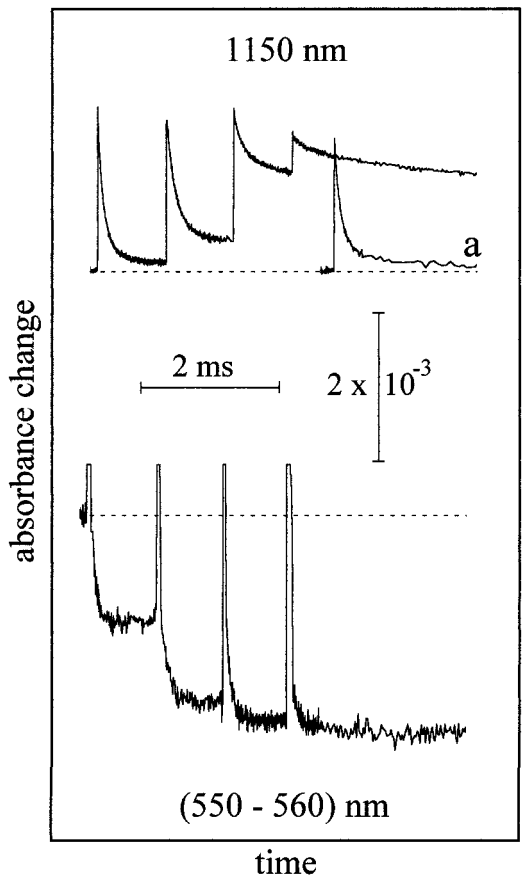

FIGURE 4: Flash-induced absorbance changes induced in four-flash experiments at 1150 nm (upper part) and 550 nm − 560 nm (lower part) in Prep-A ($A_{\approx 810} = 1.5$) in the standard reaction mixture containing 5 mM sodium ascorbate and 1.9 mM DTT. The delay between two consecutive flashes was 1 ms. The first flash was provided by a ruby laser with 13 mJ of energy, the second flash by a xenon flash, the third flash by a ruby laser with 18 mJ of energy, and the fourth flash by a Nd:YAG laser with an intensity of ≈1.5 mJ/cm^2. The first three flashes saturate RC photochemistry, while the YAG laser is about 90% saturating. The data depicted in the upper part (1150 nm) are the average of eight experiments. The signal induced by the Nd:YAG laser without preflashes is shown as a control experiment (trace a). The data depicted in the lower part are an average of four experiments recorded at both 550 and 560 nm, and the difference between these kinetics is shown. Large positive contributions presumably due mostly to ^{3}Car were observed after any flash and have been cut off for better display of the data. The absorbance changes were calculated 600 μs after each flash of the series by reference to the baseline before the first flash: -1.40×10^{-3}, -2.50×10^{-3}, -2.80×10^{-3}, and -2.90×10^{-3} after the first, second, third, and fourth flashes, respectively.

nent of cyt *c* oxidation to be probed. Examination of the $\Delta A_{(550-560)}$ signals at low excitation energies (Figure 3, bottom) shows that there is no phase of significant amplitude with a $t_{1/2}$ in the range of 3−10 μs which can be ascribed to cyt *c* oxidation, in line with measurements of P840$^+$ decay.

P840$^+$ Decay and Cyt c_{551} Accumulation during Multiple-Flash Experiments. Kinetics of P840$^+$ decay and of cyt c_{551} oxidation were studied during a series of four flashes (Δt = 1 ms between two consecutive flashes) at 1150 nm and 550 nm − 560 nm, respectively (Figure 4). With respect to RC photochemistry, the first three flashes were saturating, whereas the fourth flash (YAG laser) was not fully saturating (≈90% saturation). In this experiment, Prep-A was used despite the fact that the antenna triplet signals are larger than in Prep-B, as can be seen particularly in $\Delta A_{(550-560)}$ measurements, for which large contributions of ^{3}Car were observed. At 1150 nm (upper part), 10−15% of the decay can be ascribed to a ^{3}BChl *a* contribution for the three first flashes, whereas less than 10% is due to ^{3}BChl *a* for the fourth flash (see Figure 1). The same YAG laser flash used as a fourth flash was also used in the single-flash experiment (trace a in the upper part). The initial absorbance changes were found to be identical within 5% when the YAG laser was used either as the first or as the fourth flash (the baseline being that preceding the first flash during the four-flash experiment).

After the first and second flashes, ΔA_{1150} decays monoexponentially with a $t_{1/2}$ of about 60 and 100 μs, with amplitudes corresponding to 94 and 80% of the initial absorbance change, respectively. This is similar to what is described in Figure 2, despite some contribution of ^{3}BChl *a*. After the third flash, the fastest component has a $t_{1/2}$ of 104 μs and represents 23% amplitude. The fastest component observed after the fourth flash was difficult to fit, due to its small amplitude (<13%) because a small difference in the characteristics of the slower components leads to different estimated $t_{1/2}$ values. A halftime of about 150−250 μs was however consistently obtained in several independent measurements with different time windows used for fitting the slower components. Such microsecond components are probably due partly to reduction of P840$^+$ by cyt c_{551} and partly to ^{3}BChl *a* decay. The same experiment was performed with another sample from Prep-A with very similar results (first flash, 95% of the decay with a $t_{1/2}$ of 66 μs; second flash, 82% of the decay with a $t_{1/2}$ of 103 μs; and third flash, 23% of the decay with a $t_{1/2}$ of 106 μs). The slower components following cyt *c* oxidation were studied in another series of experiments using one to four flashes and an extended time scale. The basic characteristics of the slower components are as follows: after the first flash, a very slow decay with a $t_{1/2}$ of >200 ms; after the second flash, one component with a $t_{1/2}$ of 50−100 ms; and after the third and fourth flashes, two components with $t_{1/2}$ values of 50−100 and 5−10 ms. Possibly, all or part of these components reflect charge recombination processes. A more detailed analysis of these slow components will be reported elsewhere.

Photooxidized cyt *c* was assessed during a similar four-flash series in $\Delta A_{(550-560)}$ measurements. The kinetics of cyt *c* oxidation cannot be estimated reliably because of the large contribution of ^{3}Car signals in this sample (Prep-A). As the latter signals decay to undetectable levels after a few hundred microseconds, the amount of cyt c^+ induced by a given flash can be estimated 0.6−1.0 ms after the flash by reference to the signal level before the flash, and the total amount of photoaccumulated cyt c^+ is given by reference to the baseline preceding the first flash (dashed line). A quantitative estimate can be made by assuming that the final level after the first flash corresponds to 0.94 cyt c_{551}^+ per photoactive P840, as deduced from the decay kinetics at 1150 nm. With this assumption, the cumulative amounts of photooxidized cyt c_{551} per photoactive P840 are 0.94, 1.70, 1.92, and 1.98 after the first, second, third, and fourth flashes, respectively.

The same experiments were performed at 1150 nm and 550 nm − 560 nm with a sample from Prep-B (not shown), indicating that this sample contains about 1.5 cyt *c* molecules on average per photoactive P840 (0.91, 1.38, and 1.48

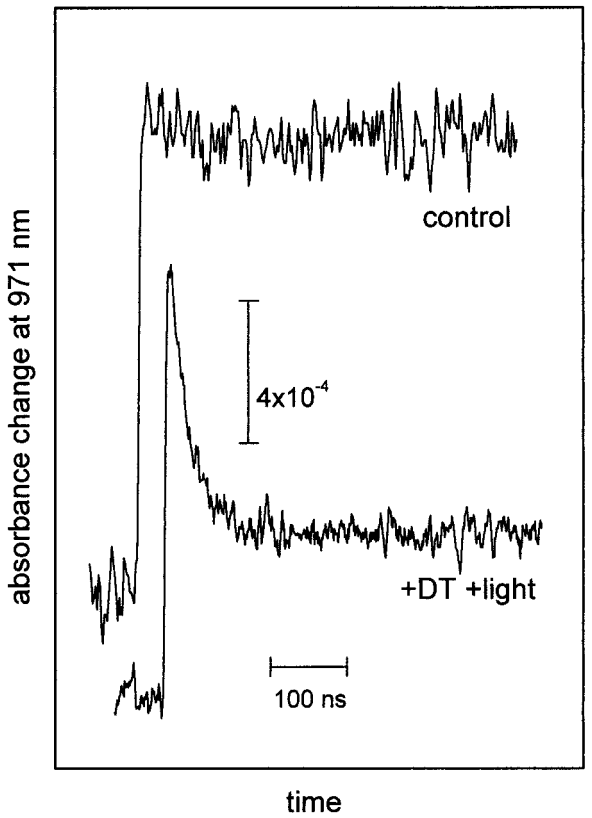

FIGURE 5: Effect of prereduction of the secondary acceptors of PS-C on the flash-induced absorbance changes at 971 nm, measured with a time resolution of 5 ns. The standard reaction mixture contained Prep-A ($A_{\approx 810} = 6$), 5 mM sodium ascorbate, and 1 μM mPMS for the control sample (upper trace). The sample that produced the lower trace contained in addition 100 μM sodium dithionite and was illuminated by white light from a projector lamp during the measurements. Repetitive (1 Hz) excitation flashes at 532 nm (about 0.5 mJ/cm^2) were provided by a 300 ps Nd:YAG laser.

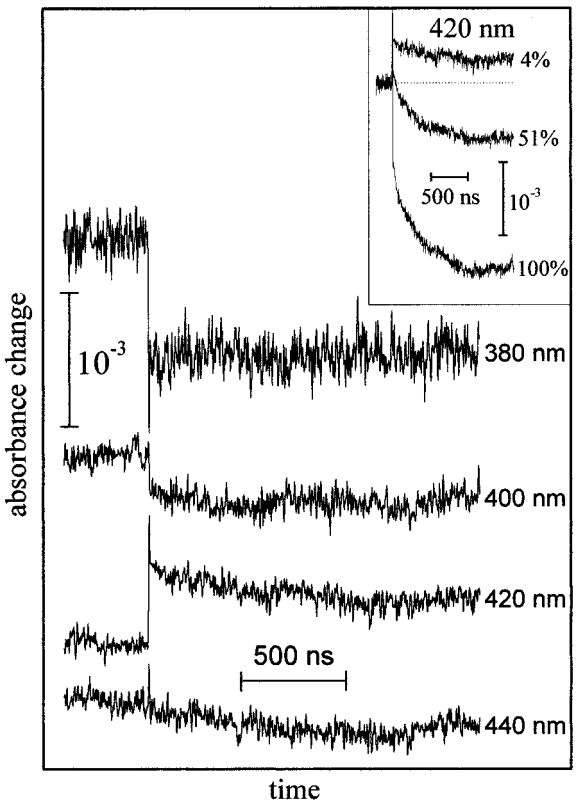

FIGURE 6: Flash-induced absorbance changes measured with a time resolution of 5 ns at the indicated wavelengths in the near-UV and blue spectral regions. The standard reaction mixture contained Prep-A ($A_{\approx 810} = 1.0$), 5 mM sodium ascorbate, 100 μM sodium dithionite, and 0.5 μM mPMS. Repetitive (1 Hz) excitation flashes at 532 nm were provided by a 300 ps Nd:YAG laser which was attenuated to 4%. The inset shows flash-induced absorbance changes at 420 nm measured with three different excitation energies. One hundred percent excitation corresponds to about 10 mJ/cm^2.

photoaccumulated cyt c^+ molecules after the first, second, and third flashes, respectively). Some cyt *c* has therefore been lost in this preparation.

P840$^+$ Decay in the Nanosecond Time Range. The upper trace of Figure 5 exhibits the absorbance change which is elicited at 970 nm by a sub-nanosecond YAG laser flash. This experiment, which was performed with a time resolution of 5 ns, shows that no transient signal, which could be ascribed to P840$^+$ decay, can be observed in the time window from 5 ns to 1 μs. To characterize the kinetics of charge recombination between the primary partners, the same measurement was performed with the same sample under a background illumination in the presence of mPMS, a photostable electron mediator, and sodium dithionite, conditions which are expected to reduce secondary electron acceptors (Figure 5, lower trace). A fast phase is clearly present under these conditions. If a single-exponential component is assumed together with an offset (for the slower decay components), $t_{1/2}$ of the fast phase was estimated to be 19 ns. The 19 ns phase accounted for 67% of the total photoinduced absorbance change, which is on the same order as that observed in the upper trace. A component with a similar short duration ($\tau = 20-35$ ns) was previously observed (*28*) and was ascribed to charge recombination between P840$^+$ and the primary acceptor in reaction centers containing no functional secondary acceptors. It was also found that the effect of the background illumination is reversible; after dark adaptation for a few minutes, about 85% of the long-lived absorbance changes observed in the control had reappeared (not shown).

Absence of Detectable Absorbance Transients Due to Menaquinone in the Near-UV and Blue Regions. Menaquinone-7 has been previously found to be associated with some PS-C preparations (*12*). Our RC preparation contained 0.6−1.2 menaquinone-7 molecules per P840 (see Materials and Methods). To detect a possible contribution of menaquinone analogous to phylloquinone A_1 of PSI, we recorded flash-induced absorbance changes between 360 and 450 nm. This spectral region was chosen because reduction of menaquinone to its semiquinone anion is accompanied by a broad absorption increase around 400 nm with a differential extinction coefficient $\Delta\epsilon$ of about 11 mM^{-1} cm^{-1} (*29*−*31*), whereas reduction of a [4Fe-4S] cluster is accompanied by a broad bleaching around 430 nm with a $\Delta\epsilon$ of more than 10 mM^{-1} cm^{-1} (see ref *32*). Hence, should electron transfer occur from reduced menaquinone to a [4Fe-4S] cluster, bleachings associated with this transfer should be observed around 400−430 nm. As a preliminary test, the dependence of flash-induced absorbance changes at 420 nm was studied in a Prep-A sample as a function of laser energy (Figure 6, inset). A strong dependence of the kinetics upon laser energy is quite evident. Whereas 100% energy leads to a large initial bleaching followed by a decaying component with a $t_{1/2}$ of

≈200 ns, a much smaller energy (4%) leads to an initial absorbance increase with little further change within 1.6 μs of flash excitation. Intermediate behaviors are observed at intermediate energies (51%). Charge separation between P840 and a reaction center acceptor, presumably an iron−sulfur cluster, has been shown to correspond to an absorption increase at 420 nm (see ref *33*). This is in line with what is observed here for a small laser energy (4%). We did not try to characterize further the larger absorbance changes observed at higher energies. These could be due to formation or decay of ^{3}BChl *a*, ^{3}Car, and ^{3}BChl$_{663}$. As a control, the YAG laser energy dependence of the flash-absorbance changes was studied at 970 nm (not shown); the biphasic dependence that was observed indicates that large antenna signals (^{3}BChl *a*) are elicited at 100% laser energy. At 4% YAG energy, it was estimated that about 50% of the RCs were undergoing charge separation. This shows that subsaturating excitation energies should be used to monitor as much as possible the true electron transfer kinetics in the blue and near-UV regions in these preparations of PS-C. Figure 6 shows typical traces measured at four different wavelengths at 4% excitation energy. Depending on the wavelength, we observed a steplike increase or decrease of absorbance. The absorbance level reached after 10 ns remained rather stable on the depicted time scale (1.6 μs) and even on an extended time scale of 4 μs (not shown). Some small decaying components are observed at 420 and 440 nm. They correspond to a $\Delta\epsilon$ of less than 5 mM^{-1} cm^{-1} (estimated by comparison with the bleaching at 830 nm observed under the same experimental conditions) and may be due to antenna components.

Effects of Preflashes on the Magnitude of Stable Charge Separation. Redox kinetics of P840 after multiple flashes were studied at 1150 nm in a Prep-A sample in the presence of mPMS and a small amount of dithionite (Figure 7). A single YAG laser flash, which was ≈90% saturating with respect to P840 photochemistry, was used for the upper trace of the left panel. For the middle trace (a), three flashes separated by 2 ms intervals were given (a saturating ruby laser flash, a saturating Xe flash, and the YAG laser flash). The lower trace (b) is the result of a four-flash experiment with a saturating preflash preceding the same three flashes used for the middle trace. Time intervals were 60, 2, and 2 ms in that case. For all three traces, the same YAG laser was used as the last flash, to compare reliably signal amplitudes. The second flash of trace b gives decay kinetics which are indistinguishable from the kinetics of the first flash, as expected if cyt c^+ is completely reduced by reduced mPMS during the 60 ms time interval. Decay kinetics are similar after the second flash in trace a and after the third flash in trace b and correspond to the second-flash kinetics which are depicted in Figure 2 (slower than after the first flash).

These identical behaviors indicate that the characteristics of P840$^+$ reduction by cyt *c* are not dependent upon the redox state of the final electron acceptors. This conclusion is also supported by the identical kinetics which are observed for the two first flashes of the lower trace of Figure 7. However, a difference was observed when comparing the last flashes of both series; whereas the initial amplitude observed after the third flash of trace a is similar to the initial amplitude observed after a single YAG laser flash, a decrease in initial

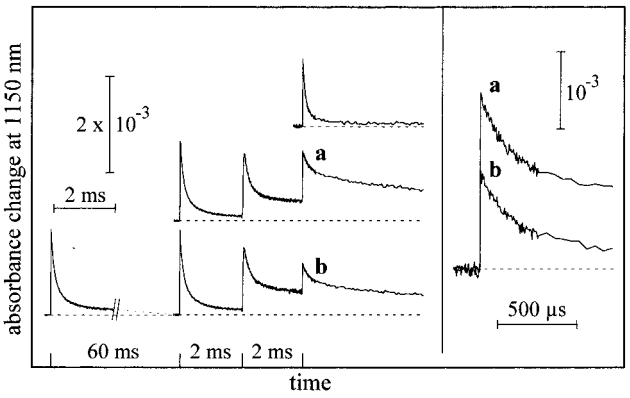

FIGURE 7: Flash-induced absorbance changes induced at 1150 nm in one-, three-, and four-flash experiments in Prep-A ($A_{\approx 810} = 1.15$) in the standard reaction mixture containing 20 μM sodium dithionite, 0.1 mM sodium ascorbate, and 0.5 μM mPMS. The upper trace of the left panel is kinetics after a single Nd:YAG laser flash (intensity of ≈1.5 mJ/cm^2). For trace a of the left panel, the same Nd:YAG laser flash was preceded by two flashes with 2 ms time spacings; the first flash was with a ruby laser (15 mJ), and the second flash was with a saturating Xe flash. For trace b of the left panel, the previous sequence of three flashes was preceded by a preflash given 60 ms before. This preflash was with a ruby laser with 13 mJ of energy. In the right panel, the last flashes of trace a (three flashes) and b (four flashes) sequences are shown on an expanded scale. The ratio of the initial amplitudes of these two signals (b/a) is 0.55. All traces correspond to averages of 36 experiments with a time interval of 15 s between the series of flashes. It was determined that there was no change related either to aging or to partial reduction of acceptors during the repetitive measurements (comparison of partial averages) and that the interval of 15 s was sufficient for complete reoxidation of accumulated acceptors (no difference in signals with time intervals of 15 and 30 s).

amplitude is observed after the fourth flash of trace b. This is better seen on an expanded time scale in the right panel of Figure 7, which shows that the signal elicited by the last flash of trace b is 60% of that of trace a.

Appearance of a Nanosecond Decaying Component after the Fourth Flash. Similar experiments were performed in the nanosecond time range by measuring redox kinetics of P840 at 970 nm. The multiple-flash excitation protocol was similar to that used in the experiment whose results are depicted in Figure 7 with a YAG laser used as the last flash. The sample was prepared in a manner similar to what is described in the legend of Figure 7 for measurements at 1150 nm, but a higher PS-C concentration was used for improving the signal-to-noise ratio. It was determined that the flashes preceding the YAG laser were saturating P840 photooxidation. The absorbance change induced by the YAG flash is shown in Figure 8. Traces 1, 3, and 4 correspond to the last flashes of the upper, middle, and lower traces of Figure 7, respectively (one-, three-, and four-flash experiments, respectively). No signal decay between 5 and 400 ns was observed on the first flash, and only a minor decay on the third flash. The smaller absorbance change of trace 3 compared to that of trace 1 is due to the fact that only 80% of P840$^+$ had been reduced (by cyt *c*) at the time of the third flash (see Figure 7). By contrast, a faster component with a $t_{1/2}$ of tens of nanoseconds and accounting for about half of the signal is observed after the fourth flash (trace 4). Despite a poorer signal-to-noise ratio than in Figure 5, it appears very likely that this fast decay is due to the same process observed during continuous background illumination ($t_{1/2}$ =

Table 1: RCs Containing Two Cyt *c* Molecules per P840[a]

redox state	$c_1\ c_2\ P$	$c_1\ c_2\ P^+$	$c_1^+\ c_2\ P$ + $c_1\ c_2^+\ P$	$c_1^+\ c_2\ P^+$ + $c_1\ c_2^+\ P^+$	$c_1^+\ c_2^+\ P$	$c_1^+\ c_2^+\ P^+$	percentage of fast phase	photoaccumulated cytochrome *c*
before flashes	100 ↘↘	0	0	0	0	0	-	-
after 1st flash	0	5.9 ↓ ↘	**94.1** ↘↘	0	0	0	**94.1**	94.1
after 2nd flash	0	0.3 (↓) ↘	**5.5** ↘↘	18.8 ↓ ↘	**75.3** ↘	0	**80.8**	174.9
after 3rd flash	0	0.0	**0.3** ↘↘	4.9 ↓ ↘	**19.5** ↘	75.3 ↓	**19.8**	194.8
after 4th flash	0	0.0	0.0	1.0	**4.2**	94.8	**4.2**	198.9

[a] Calculated equilibrium subpopulations reached after each flash of a series of four. $\Delta G^\circ = -53$ meV for electron transfer from each one of the cyt *c* molecules to P^+. The downward arrow indicates that the population of the given cell will remain, after the next flash, in the same redox state (cell just below). The lightface arrow pointing downward to the right indicates that the population will evolve, after the next flash, to the redox state corresponding to the line below and to the next column on the right. The boldface arrow pointing downward to the right indicates that the population will evolve, after the next flash, to the redox state corresponding to the line below and to the next but one column on the right. When two arrows are present in the same cell, this indicates that the given population will be distributed in two different redox states after the next flash. Bold characters refer to populations with P after the flash. On a given flash, the sum of these populations gives the percentage of the fast phase of $P840^+$ reduction.

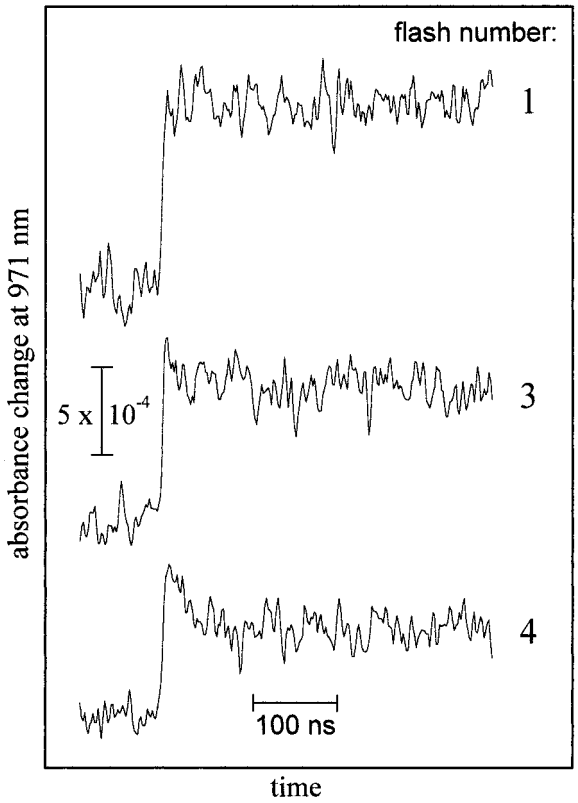

FIGURE 8: Absorbance changes at 971 nm measured with a time resolution of 5 ns induced by the last flash of a series of one (top trace), three (middle trace), and four (bottom trace) flashes spaced as in Figure 9. The excitation sources and energies were the same as in the legend of Figure 9, except that the last flash (300 ps Nd:YAG laser) was attenuated to about 0.5 mJ/cm^2. The standard reaction mixture contained Prep-A ($A_{\approx 810} = 4.6$), 5 mM sodium ascorbate, 20 μM sodium dithionite, and 0.5 μM mPMS.

19 ns). This shows that the missing amplitude observed after the fourth flash at 1150 nm with a microsecond time resolution (Figure 7) can be ascribed to a faster decay component of $P840^+$, due most probably to a recombination reaction between $P840^+$ and A_0^-.

DISCUSSION

The RC preparations from *C. tepidum* that were studied here contain a monoheme type cyt *c* similar to the cyt *c* that was identified in a RC from *C. vibrioforme* (*18*). Quinone analysis after extraction with organic solvents shows that these preparations contain 0.6−1.2 quinone molecules. The kinetics of flash-induced absorbance changes that were described above will be discussed below on one hand with regard to the behavior of cyt *c* oxidation and on the other hand with regard to the behavior of electron acceptors.

Kinetic Evidence for Two Equivalent Molecules of Monoheme Cyt c in C. tepidum Reaction Centers. A detailed kinetic study of $P840^+$ reduction and of cyt c_{551} oxidation was performed by measuring flash-induced absorbance changes at 1150 nm and 550 nm − 560 nm, respectively. The purified *C. tepidum* RCs studied here were highly photoactive as flash excitation induces almost 100% of stable charge separation, as can be seen from (a) the absence of fast recombination between $P840^+$ and the reduced primary acceptor under normal conditions (Figure 5), (b) efficient reduction of $P840^+$ by cyt *c* leading to a redox equilibrium in less than 1 ms (Figures 2−4), and (c) the very slow $P840^+$ decay ($t_{1/2} \gg 1$ ms) thereafter (Figures 4 and 7). The high photoactivity of RCs is in line with the observation that the triplet states which we observe do not saturate at high excitation energies and arise mostly from antenna pigments and not from P840, at least under normal conditions of forward electron transfer (Figure 1). The observation of a slow $P840^+$ decay ($t_{1/2} \gg 1$ ms), which is clearly seen on the third or fourth flashes, after accumulation of cyt c^+ and of two reduced acceptors (Figure 4), contrasts with some previous results, where a 70 μs phase was reported for

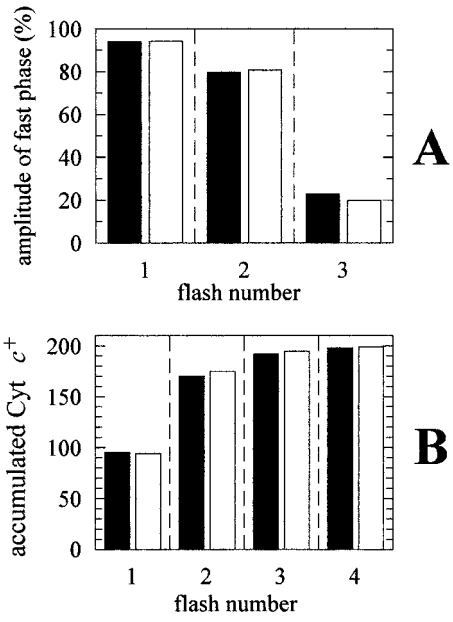

FIGURE 9: Amplitude of microsecond P840$^+$ decay (in percentage of total amplitude) (A) and of cyt c^+ accumulation (B, where a value of 100 corresponds to one photoaccumulated cyt c^+ per photoactive P840) as a function of the flash number in Prep-A. The observed values (black bars; extracted from Figure 4) are compared to the calculated values resulting from redox equilibration between P840$^+$/P840 and cyt c^+/cyt c (white bars). The model for calculations (see the text) assumes the presence of two equivalent cyt c molecules per P840 with E_m(P840$^+$/P840) − E_m(cyt$^+$/cyt) equal to 53 mV.

recombination between P840$^+$ and F_X^- (*34*). The absence of such a recombination phase, together with the only minor contribution of antenna triplet states (<15% in all ΔA_{1150} measurements shown above), allowed us to measure precisely the kinetics of P840$^+$ reduction by cyt *c*. Moreover, the measurement of photoaccumulated cyt c^+ during four-flash experiments allowed us to find that the most intact preparation contains two active cyt *c* molecules per photooxidizable P840 (Figure 4).

In the following, we will further analyze our data by comparing the sizes of the fast P840$^+$ decay phase and of photoaccumulated cyt c^+ for each flash of the series with those predicted from a minimal model based on the following assumptions. (i) The RC preparation is homogeneous with two cyt *c* molecules per P840. (ii) The free energy gap $\Delta G°$ for electron transfer from one of the two cyt *c* molecules to P840$^+$ is the same as that for electron transfer from the other cyt *c* to P840$^+$. $\Delta G°$ is independent of the redox state of the other cyt *c* and of the secondary electron acceptors.

The redox equilibrium after each flash was calculated using these assumptions (see the Appendix and Table 1). The free energy gap $\Delta G°$ was varied to fit the experimental results. The best fit was obtained with a $\Delta G°$ of −53 meV; i.e., E_m(P840$^+$/P840) − E_m(cyt$^+$/cyt) = 53 mV. Figure 9 demonstrates that the amplitudes of both fast P840$^+$ decay and photoaccumulated cyt c^+ predicted with a $\Delta G°$ of −53 meV (white bars) fit the experimental data (black bars) very well.

For a better description of the donor side of PS-C, the kinetics of cyt *c* oxidation by P840$^+$ were studied during a series of two flashes (Figure 2); under conditions which minimize the contribution of antenna ^{3}BChl *a*, P840$^+$ reduction has been found to occur with $t_{1/2}$ values of 62 (94%) and 97 μs (80%) after the first and second flashes, respectively. Another experiment carried out with a similar preparation gave $t_{1/2}$ values of 66 (95%) and 103 μs (82%), respectively. Such a flash number dependence in kinetics has not been reported previously in any PS-C preparation. As the data described above for redox equilibration after each flash of a series support the existence of two redox-equivalent cyt *c* molecules, we can further hypothesize that these cyt *c* molecules are kinetically equivalent, which leads to the following model for P840$^+$ decay after the first flash (P for P840 and c for cyt c_{551}):

Scheme 1

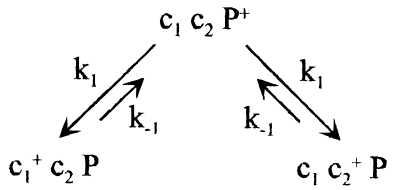

P^+ decays according to the equation $d[P^+]/dt = -2k_1[P^+] + k_{-1}([c_1^+c_2P] + [c_1c_2^+P]) = -2k_1[P^+] + k_{-1}(1 - [P^+])$, taking a value of 1 for the total PS-C population. If $[P^+] = 1.0$ at time zero (just after the flash), this leads to

$$[P^+] = 2k_1/(2k_1 + k_{-1}) \times \exp[-(2k_1 + k_{-1})t] + k_{-1}/(2k_1 + k_{-1}) \quad (1)$$

The proportion of fast P840$^+$ decay ($t_{1/2}$ of 62.5 μs), ascribed to reduction by cyt *c*, is 94% which, according to eq 1, leads to

$$2k_1/(2k_1 + k_{-1}) = 0.94 \quad \text{and}$$

$$2k_1 + k_{-1} = \ln 2/(62.5\ \mu s) = 1.11 \times 10^4\ s^{-1}$$

from which k_1 and k_{-1} can be calculated: $k_1 = 5.2 \times 10^3\ s^{-1}$ and $k_{-1} = 0.67 \times 10^3\ s^{-1}$ [from the relationship $k_1/k_{-1} = \exp(-\Delta G°/RT)$, this corresponds to $-\Delta G° = 52$ mV, which is virtually identical to the value of 53 mV which was obtained from amplitudes in the four-flash series; see above].

When the sample is excited by a second flash after establishment of the equilibrium according to Scheme 1 (1 ms after the first flash), two subpopulations should be distinguishable (see the Appendix and Table 1). The minor subpopulation ($c_1c_2P^+$) is unable to perform charge separation on the second flash and should evolve according to Scheme 1 above, leading to approximately 5.5% of fast decay with a $t_{1/2}$ of 62 μs. The major subpopulation accumulates a second positive charge on the second flash and should evolve according to Scheme 2

Scheme 2

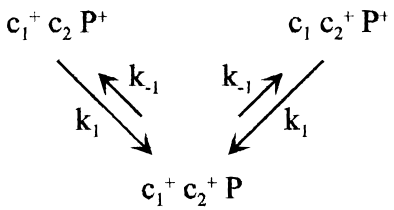

Within Scheme 2, P^+ decays according to the equation $d[P^+]/dt = -k_1[P^+] + 2k_{-1}([c_1^+c_2^+P]) = -k_1[P^+] + 2k_{-1}([P^+]_0 - [P^+])$, with $[P^+]$ equal to $[c_1^+c_2P^+] + [c_1c_2^+P^+]$ and $[P^+]_0$

being the major subpopulation ($[c_1^+c_2P^+] + [c_1c_2^+P^+]$ just after the second flash). This leads to

$$[P^+] = [P^+]_0\{k_1/(k_1 + 2k_{-1}) \times \exp[-(k_1 + 2k_{-1})t] + 2k_{-1}/(k_1 + 2k_{-1})\} \quad (2)$$

By using k_1 and k_{-1} determined from the first flash decay, the following parameters can be calculated for the P^+ decay of the major subpopulation after the second flash: $t_{1/2} = \ln 2/(k_1 + 2k_{-1}) = 106$ μs and the amount of decay $= [P^+]_0 \times k_1/(k_1 + 2k_{-1}) = 0.94 \times 0.795 = 75\%$.

Via consideration of the minor subpopulation (5.5% of $P840^+$ reduction with a $t_{1/2}$ of 62 μs), 80.5% of $P840^+$ reduction is expected from the model. This can be compared to the experimental values; 80% of $P840^+$ decays with a $t_{1/2}$ of 97 μs (monoexponential fit; see Figure 2). The close correspondence between the calculated and observed values argues in favor of the above model. The third flash decay of $P840^+$ exhibits also a fast component with a $t_{1/2}$ of 104 μs (22−23%), close to what is expected from the model (almost a single component with a rate of $k_1 + 2k_{-1}$; see also Figure 9).

A detailed comparison between $P840^+$ decay (1150 nm) and cyt c_{551} oxidation (550 nm − 560 nm) could be performed with PS-C from a preparation containing an average of 1.5 cyt *c* molecules per P840 (Prep-B) because relatively little triplet state is observed in this preparation (Figure 3). Both kinetics were shown to be very similar to each other. These $\Delta A_{(550-560)}$ measurements, taken with a 1 μs time resolution with little ^{3}Car signals, together with other measurements taken at 970 and 1150 nm with a better time resolution on a preparation containing two cyt *c* molecules per P840 (Prep-A), indicate the absence of a significant 1−10 μs component during $P840^+$ reduction by cyt *c*.

The midpoint redox potential difference of 53 mV between P840 and cyt *c*, which can explain our results according to the above schemes, is comparable to those reported previously. From redox titration of PS-C photochemistry of PS-C in membranes from "*Chloropseudomonas ethylica*", Fowler et al. (*27*) found E_m values of 240 and 170 mV for P840 and cyt *c*, respectively. Prince and Olson (*35*) found from kinetic studies that two cyt $c_{551-552}$ molecules were associated with the RC in membrane preparations from *C. limicola* with different apparent E_m values of 205 and 165 mV (250 mV for P840). They explained this difference according to Case and Parson (*36*), who reasoned that if two thermodynamically and kinetically equivalent cyt *c* molecules share one special pair, their apparent midpoint redox potential determined from titration curves of photoactive cyt *c* excited by the first and subsequent flashes will differ. More recently, Okumura et al. (*37*) reported, in a membrane preparation from *C. tepidum*, apparent E_m values of 230 mV for P840, 210 mV for the first heme, and 180 mV for the second heme.

Stoichiometry and Nature of the Cyt c Moiety in Different PS-C Preparations. Purified PS-C preparations from several laboratories contained 1.4−2.3 photooxidizable cyt *c* molecules per photoactive P840 (reviewed in ref *6*) assuming a $\Delta\epsilon$ (at α band maximum) of 20 mM^{-1} cm^{-1}, according to ref *38*. Okkels et al. (*18*) found that cyt *c* bound to PS-C from *C. vibrioforme* is a 23 kDa monoheme type cyt *c* with three deduced membrane-spanning α-helices. Oh-oka et al. (*20*, *39*) found that purified PS-C from *C. tepidum* and *C. limicola* also contained monoheme type cyt *c* whose amino acid sequence was distinctly homologous with that of *C. vibrioforme*. In the case of *C. tepidum*, it was found that two cyt *c* molecules function as electron donors to $P840^+$ (*20*). In the case of *C. limicola*, the PS-C preparation contained two copies of core polypeptide and about two cyt *c* molecules per RC. However, reduction of $P840^+$ by cyt *c* could not be studied due to the absence of functional secondary acceptors, which resulted in a fast recombination reaction between $P840^+$ and A_0^- (*39*). Kusumoto et al. (*40*) found in *C. tepidum* that the cyt *c* bound to purified PS-C is a monoheme type. However, Feiler et al. (*41*) reported that a tetraheme cyt c_{553} (32 kDa) was copurified with PS-C from *C. limicola*. It was later found that the 32 kDa heme-containing band was copurified with the RC-rich fraction up to the point of sucrose density gradient centrifugation but was subsequently removed from the latter after passage through a DEAE column (*42*). Reexamination of previously published data suggests that the same copurification behavior of tetraheme cyt *c* may hold in the case of *C. tepidum* (see Figure 1C in ref *40*). Some authors (*42*, *43*) argued that monoheme cyt *c* could be accidentally copurified with PS-C. However, this possibility seems highly unlikely in our case with two functionally equivalent and efficient cyt *c* molecules.

Hager-Brown et al. (*44*) indicated that a portion of monoheme cyt *c* could be dissociated from PS-C complexes simply by solubilizing membranes with the detergent Triton X-100 followed by sucrose density gradient centrifugation. We found that the molar ratio of photooxidizable cyt *c* to photoactive P840 was rather variable when prepared by our current protocols, and it was about 1.5 and 2.0 in PS-C preparations used in our studies. In the work presented here, our estimate of stoichiometries depends on the amounts of oxidized cyt *c* after multiple flashes and the redox equilibrium between P840 and cyt *c*, but not upon the extinction coefficents of P840 and cyt *c*, which are not precisely known. Moreover, we have been able to quantitatively explain by a simple model both the individual kinetics and the extents of cyt *c* to $P840^+$ electron transfer in a series of flashes. The model presented here involves two cyt *c* molecules with a redox potential 53 mV below that of P840. This is best explained by the presence of two geometrically equivalent cyt *c* molecules arranged with C_2 symmetry (*10*, *35*) around the homodimeric RC core (*1*, *2*, *20*).

Comparison with the Kinetics of Cyt c Oxidation Reported in the Literature. Various kinetics have been elucidated for reduction of $P840^+$ by cyt *c*. These measurements involve either purified RC, membranes, or whole cells using different strains of green sulfur bacteria (see ref *6* for a review). In some cases, a biphasic electron transfer was reported: $t_{1/2} =$ 90 and 390 μs in purified reaction centers from *C. limicola* (*10*); $t_{1/2} = 7$ and 50 μs in purified reaction centers from *C. vibrioforme* (*18*); and $t_{1/2} < 5$ and $t_{1/2} \approx 50$ μs in membrane fragments from *C. limicola* (*35*). We found that $P840^+$ reduction by cyt c_{551} is monophasic ($t_{1/2} = 62-70$ μs after the first flash), and we have no evidence of components with a significant amplitude either in the 1−10 μs time range or alternately in the hundreds of microseconds time range. From its dependence on laser excitation energy, we found that the absorbance change kinetics in the hundreds of microseconds time range that is observed in our samples can be ascribed

to ^{3}BChl (see Materials and Methods). The assignment of a 7 μs phase to cyt *c* oxidation made in ref *18* is disputable as these data show a major contribution of fast decaying ^{3}Car signals which make a large contribution at 551 nm (see ref *25*). ^{3}Car might also explain the $t_{1/2} < 5$ μs component observed in ref *35*.

With respect to an alternative explanation, we cite a recent study relying upon flash-induced absorbance measurements at different temperatures and viscosities. Oh-oka et al. (*19*) proposed a model with conformational fluctuations of the heme-containing moiety of cyt *c* in PS-C. In the framework of this model, the observed electron transfer kinetics should generally be rather complex. As a simplified version of the model, we can postulate a proximal site of heme association with the RC core, electron transfer occurring only in this conformation. If this model is correct, a monoexponential electron transfer can be observed only in two cases; the conformational fluctuations are faster than electron transfer with cyt *c* in the proximal site, or the probability of finding the cyt *c* in this site is very small. If these conditions are not met, a multiphasic decay is expected, with the fastest component corresponding to electron transfer with cyt *c* in the proximal site. Such a situation may arise depending upon the experimental conditions (pH, ionic strength, temperature, and viscosity) and thus may lead to a biphasic behavior as observed in ref *35*.

A Quinone Acceptor Cannot Be Detected by Flash-Induced Absorbance Kinetics. The presence of quinones in purified PS-C is controversial (see the introductory section). We found that PS-C prepared with Triton X-100 contained significant amounts of menaquinone-7, and its content was estimated by reference to $BChl_{663}$ to be 0.6−1.2 molecules per RC assuming that each PS-C contains six (*21*) to nine (*12*) $BChl_{663}$ molecules per RC, respectively. Although we do not know why the menaquinone-7 content differs among PS-C preparations from different groups, our results indicate that the absence of menaquinone-7 in some PS-C preparations solubilized with Triton (*45*) is not merely due to the choice of the detergent. Strict anaerobic conditions during PS-C preparations may be necessary for conserving quinones. On the other hand, we cannot exclude the possibility that menaquinone detected in our RC preparations is a contamination from menaquinone present in the membrane.

Involvement of a quinone in electron transfer in green sulfur bacteria and heliobacteria also remains controversial (see the introductory section). Reoxidation of A_0^- during forward electron transfer has been observed in membranes of the green sulfur bacterium *Prosthecochloris aestuarii* with a τ of ≈700 ps (*46*), but the partner of A_0^- during this reaction was not identified. Though menaquinone is present in our samples, our kinetic data provide several lines of evidence that do not support its involvement in forward electron transfer.

(a) We were looking for absorbance transients in the UV and blue regions that would occur in the time window from 5 ns to 4 μs. Under subsaturating conditions of light excitation, only very small transients could be observed, meaning that menaquinone cannot be detected during forward electron transfer in the corresponding time window.

(b) Multiple-flash experiments were performed at 970 and 1150 nm which were aimed at counting the number of stable secondary acceptors (Figures 7 and 8). These experiments made use of the presence of two fast-donating cyt *c* molecules per P840 in photoaccumulating reduced acceptors within a short time range. When two acceptors were prereduced to a large extent by the first two flashes, $P840^+$ decayed in the microsecond to millisecond time range after the third flash. Most, if not all, of the microsecond decay of $P840^+$ can be ascribed to reduction of $P840^+$ by some cyt *c* which remains oxidized after the second flash, whereas a recombination reaction between $P840^+$ and a third reduced acceptor is occurring on a slower time scale. This is in accordance with the presence of three relatively stable electron acceptors, which are presumably the three iron−sulfur clusters which are thought to be present in RCs of green sulfur bacteria (see ref *6* for a review). During four-flash experiments, we made use of an efficient electron donor (mPMS) and a relatively long time interval (60 ms), allowing us to fully reduce P840 and cyt *c* between the first and second flashes. In that way, it was possible to observe the effect of the fourth flash, after having photoaccumulated three reducing equivalents in the acceptor side after the first three flashes. Under these conditions, a fast decay phase with a $t_{1/2}$ of ≈20 ns is occurring after the fourth flash, whereas such a phase is insignificant following the preceding flashes. This fast phase is mirrored in a decreased signal amplitude observed after the fourth flash and recorded at 1150 nm with a 4 μs time resolution. These results therefore indicate that the acceptor side of our PS-C preparation can stabilize only three electrons. Although the precise content of iron−sulfur clusters in our preparations has not been evaluated and the EPR signal of the third iron−sulfur cluster (the counterpart of F_X in PSI) remains rather elusive, we propose that the third stable acceptor in our preparation is F_X and that, when three acceptors have been prereduced, the fourth excitation reduces A_0 as the terminal acceptor.

The rate of A_0^- reoxidation during forward electron transfer is reduced about 20-fold in PS-C compared to that in PSI (*46*; see ref *7* for a review of PSI reactions). If quinone is not an intermediate electron carrier between A_0 and F_X in green sulfur bacteria, one could have expected a larger decrease in the rate in view of the strong distance dependence of the electron transfer rate (*47*, *48*). This may indicate that the edge to edge distance between A_0 and F_X is somewhat shorter in green sulfur bacteria than in PSI. Though our results oppose the view that quinone is involved in forward electron transfer, one can think about the possibilities that remain for the involvement of menaquinone during electron transfer in PS-C; it may have escaped detection by flash-absorbance measurements, for instance, because it is reoxidized faster than it is reduced (or is in very fast redox equilibrium with F_X). In addition, its reduction may be prevented when the three iron−sulfur clusters have been prereduced, possibly through the electrostatic effects on its redox potential.

APPENDIX

In the following, PS-C is considered to contain two equivalent cyt *c* molecules, named c_1 and c_2, per P840 (P). The standard free energy change $\Delta G°$ for electron transfer from each one of the cyt *c* molecules to P^+ is independent of the redox states of the other cyt *c* molecules and the secondary electron acceptors.

After equilibrium had been established following the first flash (Scheme 1), $([c_1^+c_2P]_{eq} + [c_1c_2^+P]_{eq})/[c_1c_2P^+]_{eq} = 2k_1/k_{-1} = 2\exp(-\Delta G°/k_BT)$, where the subscript eq stands for "at equilibrium" and k_B is the Boltzmann constant.

Using $A = \exp(-\Delta G°/k_BT)$, one obtains for the proportion p_1 with the positive charge on one of the cyt *c* molecules the equation $p_1 = ([c_1^+c_2P]_{eq} + [c_1c_2^+P]_{eq})/([c_1^+c_2P]_{eq} + [c_1c_2^+P]_{eq} + [c_1c_2P^+]_{eq}) = (2A)/(2A + 1)$, and for the complementary proportion $(1 - p_1)$, the positive charge is on P ($c_1c_2P^+$).

The second flash elicits a charge separation only in the subpopulation with P reduced, resulting in two positive charges on the donor side.

This subpopulation (proportion p_1) will evolve after the second flash according to Scheme 2 and establish the following equilibrium:

$$[c_1^+c_2^+P]_{eq}/([c_1^+c_2P^+]_{eq} + [c_1c_2^+P^+]_{eq}) = k_1/2k_{-1} = 0.5\exp(-\Delta G°/k_BT)$$

Hence, for the proportion p_2 with both positive charges on cytochromes:

$$p_2 = [c_1^+c_2^+P]_{eq}/([c_1^+c_2^+P]_{eq} + [c_1^+c_2P^+]_{eq} + [c_1c_2^+P^+]_{eq}) = A/(A + 2)$$

For the complementary proportion $(1 - p_2)$, one positive charge is on one of the cyt *c* molecules and the other one on P ($c_1^+c_2P^+$ and $c_1c_2^+P^+$).

The subpopulation with P^+ at the time of the second flash (proportion $1 - p_1$) has only one positive charge on the donor side. It will evolve after the second flash according to the equilibrium described above for the first flash: proportion $p_1 = (2A)/(2A + 1)$ of the RC with the positive charge on one of the cyt *c* molecules and proportion $1 - p_1$ with the positive charge on P.

At equilibrium following the second flash, there will therefore be four different subpopulations: p_1p_2 in state $c_1^+c_2^+P$, $p_1 \times (1 - p_2)$ in states $c_1^+c_2P^+$ and $c_1c_2^+P^+$, $(1 - p_1)p_1$ in states $c_1^+c_2P$ and $c_1c_2^+P$, and $(1 - p_1)^2$ in state $c_1c_2P^+$.

The same type of calculation can be carried out for the third flash, resulting in five different subpopulations: p_1p_2 in state $c_1^+c_2^+P^+$, $p_1(1 - p_2)(2 - p_1 - p_2)$ in states $c_1^+c_2P^+$ and $c_1c_2^+P^+$, $p_1p_2(2 - p_1 - p_2)$ in state $c_1^+c_2^+P$, $(1 - p_1)^2 \times p_1$ in states $c_1^+c_2P$ and $c_1c_2^+P$, and $(1 - p_1)^3$ in state $c_1c_2P^+$.

For the fourth flash, one obtains five different subpopulations (only the first three being significantly populated assuming $\Delta G° = -53$ meV): $p_1p_2(3 - p_1 - p_2)$ in state $c_1^+c_2^+P^+$, $p_1(1 - p_2)[(1 - p_2)(2 - p_1 - p_2) + (1 - p_1)^2]$ in states $c_1^+c_2P^+$ and $c_1c_2^+P^+$, $p_1p_2[(1 - p_2)(2 - p_1 - p_2) + (1 - p_1)^2]$ in state $c_1^+c_2^+P$, $p_1(1 - p_1)^3$ in states $c_1^+c_2P$ and $c_1c_2^+P$, and $(1 - p_1)^4$ in state $c_1c_2P^+$.

A numerical example is given in Table 1 assuming $\Delta G° = -53$ meV and $k_BT = 25.5$ meV, which gives a p_1 of 0.941 and a p_2 of 0.800.

ACKNOWLEDGMENT

We thank Dr. M. Mochimaru for collaboration in quinone analysis and Mr. D. Nakazato for collaboration in preparing PS-C.

REFERENCES

1. Buettner, M., Xie, D. L., Nelson, H., Pinther, W., Hauska, G., and Nelson, N. (1992) *Proc. Natl. Acad. Sci. U.S.A. 89*, 8135.
2. Buettner, M., Xie, D. L., Nelson, H., Pinther, W., Hauska, G., and Nelson, N. (1992) *Biochim. Biophys. Acta 1101*, 154.
3. Liebl, U., Mockensturm-Wilson, M., Trost, J. T., Brune, D. C., Blankenship, R. E., and Vermaas, W. (1993) *Proc. Natl. Acad. Sci. U.S.A. 90*, 7130.
4. Golbeck, J. H. (1993) *Curr. Opin. Struct. Biol. 3*, 508.
5. Feiler, U., and Hauska, G. (1995) Advances in Photosynthesis 2, in *Anoxygenic Photosynthetic Bacteria* (Blankenship, R. E., Madigan, M. T., and Bauer, C. E., Eds.) pp 665−685, Kluwer Academic Publishers, Dordrecht, The Netherlands.
6. Sakurai, H., Kusumoto, N., and Inoue, K. (1996) *Photochem. Photobiol. 64*, 5.
7. Brettel, K. (1997) *Biochim. Biophys. Acta 1318*, 322.
8. Kleinherenbrink, F. A. M., Ikegami, I., Hiraishi, A., Otte, S. C. M., and Amesz, J. (1993) *Biochim. Biophys. Acta 1142*, 69.
9. Brettel, K., Leibl, W., and Liebl, U. (1998) *Biochim. Biophys. Acta 1363*, 175.
10. Oh-oka, H., Kakutani, S., Matsubara, H., Malkin, R., and Itoh, S. (1993) *Plant Cell Physiol. 34*, 93.
11. Frankenberg, N., Hager-Braun, C., Feiler, U., Fuhrmann, M., Rogl, H., Schneebauer, N., Nelson, N., and Hauska, G. (1996) *Photochem. Photobiol. 64*, 14.
12. Kjaer, B., Frigaard, N. U., Yang, F., Zybailov, B., Miller, M., Golbeck, J. H., and Scheller, H. V. (1998) *Biochemistry 37*, 3237.
13. Nitschke, W., Feiler, U., Lockau, W., and Hauska, G. (1987) *FEBS Lett. 218*, 283.
14. Muhiuddin, I. P., Rigby, S. E. J., Evans, M. C. W., and Heathcote, P. (1995) in *Photosynthesis: from Light to Biosphere. Proceedings of the Xth International Congress of Photosynthesis* (Mathis, P., Ed.) Vol. II, pp 159−162, Kluwer Academic Publishers, Dordrecht, The Netherlands.
15. Kusumoto, N., Inoue, K., Nasu, H., and Sakurai, H. (1994) *Plant Cell Physiol. 35*, 17.
16. Scott, M. P., Kjoer, B., Scheller, H. V., and Golbeck, J. H. (1997) *Eur. J. Biochem. 244*, 454.
17. Hager-Braun, C., Jarosch, U., Hauska, G., Nitschke, W., and Riedel, A. (1997) *Photosynth. Res. 51*, 127.
18. Okkels, J. S., Kjaer, B., Hansson, Ö., Svendsen, I., Lindberg Møller, B., and Scheller, H. V. (1992) *J. Biol. Chem. 267*, 21139.
19. Oh-oka, H., Iwaki, M., and Itoh, S. (1997) *Biochemistry 36*, 9267.
20. Oh-oka, H., Kamei, S., Matsubara, H., Iwaki, M., and Itoh, S. (1995) *FEBS Lett. 365*, 30.
21. Kobayashi, M., van de Meent, E. J., Ohoka, H., Inoue, K., Itoh, S., Amesz, J., and Watanabe, T. (1992) in *Research in Photosynthesis. Proceedings of the 9th International Congress of Photosynthesis* (Murata, N., Ed.) Vol. I, pp 393−396, Kluwer Academic Publishers, Dordrecht, The Netherlands.
22. Olson, J. M., Prince, R. C., and Brune, D. C. (1976) *Brookhaven Symp. Biol. 28*, 238.
23. Gerken, S., Brettel, K., Schlodder, E., and Witt, H. T. (1987) *FEBS Lett. 223*, 376.
24. Shuvalov, V. A., and Parson, W. W. (1981) *Biochim. Biophys. Acta 638*, 50.
25. Franken, E. M., and Amesz, J. (1997) *Biochim. Biophys. Acta 1319*, 214.
26. Beechem, J. M. (1992) *Methods Enzymol. 210*, 37.
27. Fowler, C. F., Nugent, N. A., and Fuller, R. C. (1971) *Proc. Natl. Acad. Sci. U.S.A. 68*, 2278.
28. Van Bochove, A. C., Swarthoff, T., Kingma, H., Hof, R. M., Van Grondelle, R., Duysens, L. N. M., and Amesz, J. (1984) *Biochim. Biophys. Acta 764*, 343.
29. Rao, P. S., and Hayon, E. (1973) *Biochim. Biophys. Acta 292*, 516.
30. Romijn, J. C., and Amesz, J. (1977) *Biochim. Biophys. Acta 461*, 327.

31. Shopes, R. J., and Wraight, C. A. (1985) *Biochim. Biophys. Acta 806*, 348.
32. Ke, B. (1973) *Biochim. Biophys. Acta 301*, 1.
33. Swarthoff, T., Van der Veek-Horsley, K. M., and Amesz, J. (1981) *Biochim. Biophys. Acta 635*, 1.
34. Miller, M., Liu, X., Snyder, S. W., Thurnauer, M. C., and Biggins, J. (1992) *Biochemistry 31*, 4354.
35. Prince, R. C., and Olson, J. M. (1976) *Biochim. Biophys. Acta 423*, 357.
36. Case, G. D., and Parson, W. W. (1988) *Biochim. Biophys. Acta 253*, 187.
37. Okumura, N., Shimada, K., and Matsuura, K. (1994) *Photosynth. Res. 41*, 125.
38. Olson, J. M., Giddings, T. H., Jr., and Shaw, E. K. (1976) *Biochim. Biophys. Acta 449*, 197.
39. Oh-oka, H., Kakutani, S., Kamei, S., Matsubara, H., Iwaki, M., and Itoh, S. (1995) *Biochemistry 34*, 13091.
40. Kusumoto, N., Inoue, K., Nasu, H., Tomioka, A., and Sakurai, H. (1995) in *Photosynthesis: from Light to Biosphere. Proceedings of the Xth International Congress of Photosynthesis* (Mathis, P., Ed.) Vol. II, pp 203−206, Kluwer Academic Publishers, Dordrecht, The Netherlands.
41. Feiler, U., Nitschke, W., and Michel, H. (1992) *Biochemistry 31*, 2608.
42. Albouy, D., Sturgis, J. N., Feiler, U., Nitschke, W., and Robert, B. (1997) *Biochemistry 36*, 1927.
43. Albouy, D., Joliot, P., Robert, B., and Nitschke, W. (1997) *Eur. J. Biochem. 249*, 630.
44. Hager-Braun, C., Xie, D. L., Jarosch, U., Herold, E., Buettner, M., Zimmermann, R., Deutzmann, R., Hauska, G., and Nelson, N. (1995) *Biochemistry 34*, 9617.
45. Hager-Braun, C., Frigaard, N.-U., Permentier, H. P., Schmidt, K. A., Hauska, G., Amesz, J., and Miller, M. (1998) in *Photosynthesis: Mechanisms and Effects. Proceedings of the XIth International Congress of Photosynthesis* (Garab, G., Ed.) Vol. I, pp 555−558, Kluwer Academic Publishers, Dordrecht, The Netherlands.
46. Shuvalov, V. A., Vasmel, H., Amesz, J., and Duysens, L. N. (1986) *Biochim. Biophys. Acta 851*, 361.
47. Marcus, R. A., and Sutin, N. (1985) *Biochim. Biophys. Acta 811*, 265.
48. Moser, C. C., Keske, J. M., Warncke, K., Farid, R. S., and Dutton, P. L. (1992) *Nature 355*, 796.

BI990452S